

Colour local pattern: a texture feature for colour images

Noël Richard, Armando Martínez Ríos¹ and Christine Fernandez-Maloigne

Université de Poitiers, XLIM UMR CNRS 7252, France

¹Instituto Politécnico Nacional México, Mexico

Email: noel.richard@univ-poitiers.fr

The Julesz's conjectures were the foundations for the development of many methods for texture discrimination as spatial arrangements of local patterns. These local patterns represent a bridge between a first conjecture that handles a purely statistical approach and the texton theory. Beyond the mathematical construction of the Local Binary Patterns (LBP) proposed by Ojala, the proposed pattern defined by a circular neighbourhood can be considered as texton. Nevertheless, the binarisation step inside the Local Binary Pattern reduced the ability to be sensitive to the details of high spatial frequencies. In addition, the colour extension of Local Binary Pattern is not straightforward. In this article, we introduce the Colour Local Patterns (CLP) as a new vector texture feature able to characterise colour texture. The Colour Local Pattern inherits from the Local Binary Pattern construction and from the psycho-physical results, starting from the third Julesz's conjecture. By defining the CLP in a perceptual colour space and by using a perceptual distance, we embed the notion of neighbourhood defined by Julesz and used in LBP. Then by applying a Fourier transform, we generate a signature vector for the local signature. The results achieved in classification tasks are higher around 10% in the rate of good classification in two databases with the largest number of images.

Received 01 March 2016; revised 27 June 2016; accepted 04 July 2016

Published online: 3 August 2016

Introduction

The human visual system (HVS) processes the visual information by extracting the salient regions from their local contrast in the perceived sense. In this process, the information of texture and colour takes an important place [1]. There are two functionally different visual information-processing systems. The first one, the pre-attentive system, processes the visual information at the pre-conscious level and without the help of cognitive process. The second one, the attentive system, involves search, research and cognitive processing. The pre-attentive system separates the regions of a figure with the background, acting thus as a guide for the attentive system which is responsible of object identification [2].

There are many theories to set the way in which the human visual system encodes the structure of an image in the pre-attentive system [3]. Julesz in the first conjecture proposed it, by means of differences statistics of first and second order that contribute at the discrimination [4]. Later he wide this conjecture: “*whereas textures that differ in their first and second-order statistics can be discriminated from each other, those that differ in third-order or higher order usually cannot*”. More complex relationship information are required to solve these limits [5].

The second part of the Julesz’s work developed with Caelli established that the textures are easily discriminable by a number of geometric properties as local curvatures, endpoints and junctions called “*perceptive quarks*” [6]. After, Bergen and the same Julesz expanded this definition in the *texton* theory. This theory stated that discrimination is due to the first-order statistical differences between *textons*. *Textons* are generally reduced to segments of lines with specific length, orientation, width and gap, as well as terminations, crosses and blobs [7].

In parallel, the foundations of texture assessment by image processing tools started with Haralick, who translated the Julesz’s purposes into the co-occurrence construction [8]. Since these works, lot of methods were developed for intensity images, to express the texture information into digital features (histogram difference, co-occurrence, run-length matrix, Fourier transformations, local binary patterns,...).

However, the extension to colour images is not straightforward. The first constructions followed the Poirson and Wandell’s hypothesis [9] proposing to separate the colour information from the texture [10-12]. Nevertheless, such hypothesis is too basic in front of the spatio-chromatic complexity of natural images. So Palm’s proposed to process the texture information on each colour channel (marginal construction) and to combine them into a single texture feature. To take into account the inter-channel dependency, Arvis added to the marginal construction the inter-channel texture information [12-13]. Recently, Martínez Ríos *et al.* showed that for natural images vector model of colour texture assessment are more accurate in texture discrimination. They argued that the right texture model for colour images depends on the inner spatio-chromatic complexity of the image [14]. Consequently, they extended the basic approaches separating the colour and the texture to the vector models including naturally the two aspects [15].

Our work proposes to show how to adapt the Local Binary Pattern in the context of colour images respecting the *texton* model from Julesz and using perceptual colour distances. We will show how to avoid the limitations of LBP due to the binarisation step and how to preserve the LBP advantages in texture characterisation/discrimination due to the word histograms. This paper is organised as follow: in the following section, the mathematical definition of Local Binary Pattern is recalled. Then, we develop the Colour Local Pattern (CLP) construction and the associated feature. In the section Results and Discussion, we analyse the CLP behaviour in front of 4 sets of images coming from the most used databases in colour texture classification contests. Finally we compare the performance in texture classification of CLP in front of the colour extension of LBP. Then endings and next trends are developed as conclusions.

Local binary pattern

Local Binary Pattern (LBP) was proposed by Ojala *et al.* for texture recognition and classification of grey-level images [16]. Later several authors adapted it for colour texture assessments [17]. The original algorithm presents a low computational complexity and a low sensitivity to changes in illumination [18].

Due to the initial construction, LBP can be considered as a bridge between statistical models and structural models of texture analysis [19]. Therefore, Huang defines LBP as *the quantification of the statistical occurrences of individual patterns invariant to rotation corresponding to certain micro-textures on the image*; consequently, patterns can be considered as a feature detector [20]. LBP approaches have been proposed originally for texture classification but are applied also for face image analysis, image and video retrieval, environment modelling, visual inspection and biomedical image analysis [20-21].

The initial mathematic definition of LBP is divided in two parts, first one extracts the local binary patterns from an intensity image and the second one processes a pattern histogram for texture discrimination purposes [21]. In the following, we recall these two steps.

Definition of local binary pattern

The local pattern $T_{p,d}(x)$ is defined at the x location by the sequence of the local differences between $I(x)$ and the neighbored values $I(p)$. The neighbourhood is defined for a spatial localisation x , considering a set of P neighbored pixels at a distance d from x :

$$T_{p,d}(x) = \{(I(p) - I(x)), \forall p \in [0, P - 1]\} \quad (1)$$

where $p = x + de^{ik\frac{2\pi}{P}}$

Local binary pattern histogram

Ojala works with histograms of words H_w^d for texture characterisation. The considered words $W_i^d(x)$ are obtained by the sequence of the binarised differences from the local pattern. The final result is an integer due to the binary word transformation into an unsigned value. Equation 2 shows the word construction using a *weighting* in power of two of the local difference and the final summation.

$$W_i^d(x) = \sum_{p=0}^{P-1} \text{Sign}(I(p) - I(x))2^p \quad (2)$$

and $S(c) = \begin{cases} 1, & \forall c \geq 0 \\ 0, & \forall c < 0 \end{cases}$

Finally, the texture signature is defined by the histograms of words $W_i^d(x)$:

$$\text{Sig}(I) = H_w^d(I) = \{\text{prob}(W_i^d = a), \forall a \in [0, 2^P - 1]\} \quad (3)$$

From the colour extension

The colour extension of LBP into the colour domain is classically developed following two different ways. The first one splits the colour texture into a texture information processed from an intensity image and combined with colour statistics (Grey-Level Approaches with Colour Information: GLACI). The second one processes the colour texture thanks to grey-level texture features applied on each colour channel (C_1, C_2, C_3) in a separated processing (marginal approach). Arvis proposed to improve this approach adding the texture assessment between channel ($C_i \rightarrow C_j$ with $i \neq j$). This approach is known as *Cross-Channel Marginal Approach* (CCMA). In this last case, the corresponding distributions are thus represented in nine different histograms: three intra-component features: C_1-C_1, C_2-C_2 , and C_3-C_3 and six inter-component features: $C_1-C_2, C_2-C_1, C_1-C_3, C_3-C_1, C_2-C_3$ and C_3-C_2 .

Consequently a colour texture is characterised using LBP by 9 histograms of 256 words [10]. Porebsky proposed a method of feature selection to reduce the size of the resulting vector and to improve the good classification rates [17].

The CLP mathematic definition

To be close from the Julesz's conjecture and to the models of human perception, the Colour Local Pattern (CLP) must be defined using perceptual distance. So the circular neighbourhood sequence must be defined by the vector colour difference $\vec{s}(k)$ calculated in a colour space like CIE L*a*b*. The circular neighbourhood is sampled by a factor P to manage the discrete angular θ :

$$\vec{s}(k) = I_L(p) - I_L(x), \forall p \in [0, P - 1] \quad (4)$$

$$\text{with } p = x + d \cdot e^{ik \frac{2\pi}{P}} \Rightarrow \theta = k \frac{2\pi}{P}$$

In the Equation 4, $I_L(x)$ is the transformed coordinate of $I(x)$ in the adapted colour space (CIE L*a*b* or another colour space where a perceptual colour distance is enabled). To define an efficient feature from the $\vec{s}(k)$ sequence, the Fourier transform $S_{p,d}(\theta)$ of the sequence $\vec{s}(k)$ is processed. To stay close from known LBP standard, the vector construction of this difference was built in two parts, first one considers the norm of this difference using a perceptual distance in an adapted colour space. The second one considers the orientation of this difference in this adapted colour space. Consequently, the Fourier analysis of the difference pattern was developed on three scalar values expressing the vector nature of the sequence $\vec{s}(k)$: a norm and two angles (to see Equation 5).

$$\vec{s}(k) = \begin{cases} |\vec{s}(k)| = \Delta E(I_L(p), I_L(x)) \\ \perp \vec{s}(k) = \perp(\vec{Oa}, \vec{s}(k)) = (\alpha(k), \beta(k)) \end{cases} \quad \forall p \in [0, P - 1] \text{ and } I_L(x) \in \text{CIE L*a*b*} \quad (5)$$

Colour local pattern feature

The main interest of the Ojala's construction for LBP was to transform the distance between texture signatures into a distance between histogram of words. In a similar manner, the distance between CLP features will be based on distance between distributions coming from the Fourier transform of the norm and angle of $\vec{s}(k)$.

In a first consideration, we limit the CLP feature to the norm of the Fourier transform of $\vec{s}(k)$ (equation 6). Keeping the square of the norm, the feature is correlated to a power measure, thanks to that the first feature value ($V=0$) expresses the average colour distance between the pixel location x and the pixels values on the neighbourhood.

In addition, as $s(k)$ is a real function, we can store half part of the spectrum.

$$sig_{clp\Delta}(I) = \left\{ (S_{p,d}^I(V))^2, \forall V \in [0, P/2] \right\} \quad (6)$$

Results and Discussion

Dataset and graphics results

This sub-section presents some texture signatures for images from *OUTEX*, *VISTEX*, *STEX* and *ALOT* databases. The texture signatures are the average CLP features.

The physical and perceptual constraints in Julesz conjecture on spatial distances require to work with Euclidean distances to produce an anisotropic analysis. So to preserve the circularity constraint induces by the Euclidean distance and taking into account the requirement of a small distance, we selected a radius of 3 pixels, approximating the circle by an octagon of 16 pixels ($d=3$ and $P=16$ in Equation 4). Such a choice allows also to be in concordance with the FFT requirements.

CLP features for some OUTEX images

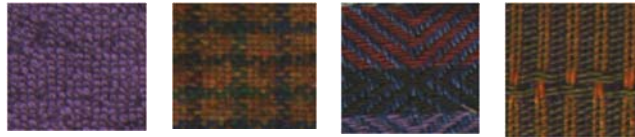


Figure 1: Some images of colour texture from OUTEX test; left to right – Canvas 2, Canvas 4, Canvas 20 and Wool 4 (there are totally 68 images captured under the same illumination conditions).

OUTEX test is the "TC 00013" with 68 colour texture images of 746×538 pixels of 24 bits. Following Arvis for the classification process, images are split up into 20 disjoint sub-images of 128×128 pixels producing 20 sub-images. Each initial image is associated to one class, the complete image set generates 1360 sub-images, 50% for to learn and the rest for classification. The Figure 1 shows some images of this database and the Figure 2 the associated CLP signature.

The magnitude of the signature for the null frequency is relative to the average distance in the local neighbourhood. More important is this value, more homogeneous is the texture content (Canvas 2). Without logarithmic weighting, the magnitude variations far from the null frequency is reduced, nevertheless differences appears at these high frequencies between textures (Canvas 20 vs Wool 4 typically).

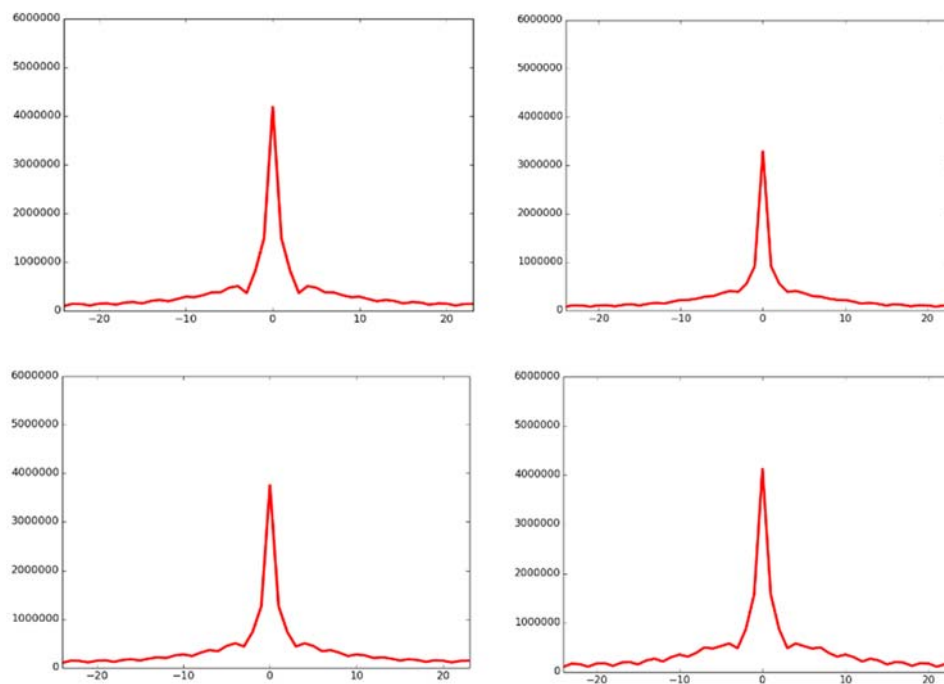


Figure 2: Colour local pattern amplitude from OUTEX test – Canvas 2 (top left), Canvas 4 (top right), Canvas 20 (bottom left) and Wool 4 (bottom right).

CLP features for some VISTEX images

VISTEX test is based on the image set labelled "Contrib TC 0006", with 54 colour texture images, whose initial size are 512×512 pixels. As for the OUTEX case, the images are split into 16 disjoint sub-images of size 128×128 pixels (Figure 3). Thus 432 images are used to build the learning subset and the 432 remaining are used to build the classification feature vector.

Unlike the OUTEX database, the signature variations between textures are more important reflecting the variety in colour and texture aspect of the representative images (Figure 4). In particular, the CLP magnitude of image *fabric* is the most important of the four VISTEX cases. By opposition, the curve corresponding to the figure *bark* presents the lowest amplitude and minor variations outside the null frequency. In this last case the radius used to define the spatial neighbourhood is too small ($d=3$) in front of the size of the image.



Figure 3: Some images of colour texture from VISTEX test; left to right – Food, Flower, Bark and Fabric (there are totally 54 images captured under different illumination conditions, they are very different in contents and viewing conditions).

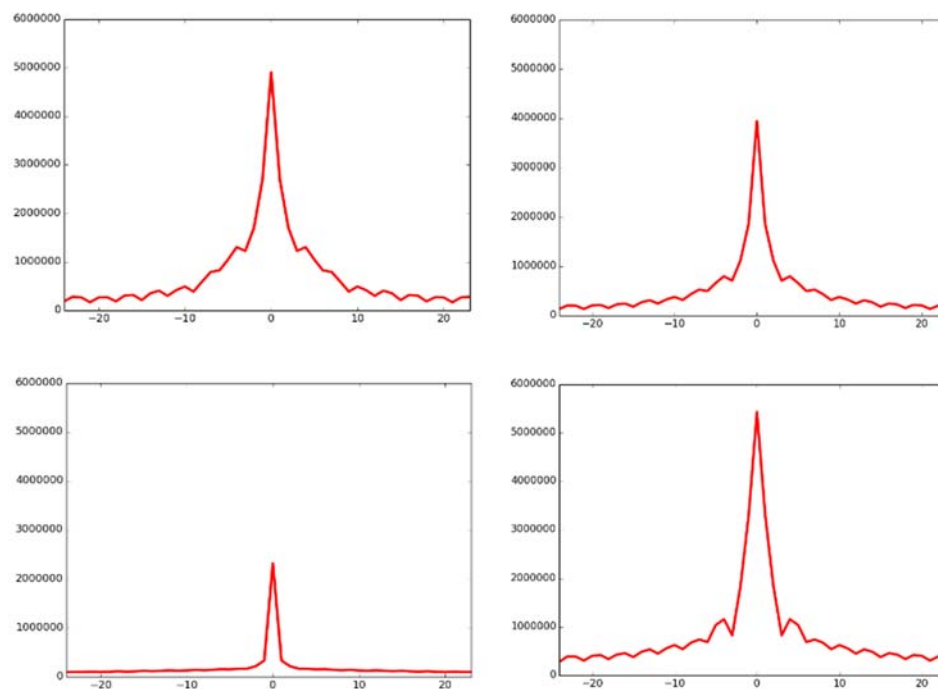


Figure 4: Colour local pattern amplitude from VISTEX test – Food (top left), Flower (top right), Bark (bottom left) and Fabric (bottom right).

CLP features for some STEX images

STEX database is based on the image set labelled "Salzburg texture image database". It includes 476 colour texture images, whose initial size are 512×512 pixels; the authors didn't describe the acquisition conditions. The image content induces uncontrolled viewing and illumination conditions.



Figure 5: Some images of colour texture from *STEX* test; left to right – *Bark 01*, *Bush 08*, *Tree 05* and *Wood 30* (there are totally 476 images captured under different illumination conditions, they are very different in contents and viewing conditions).

Inside the *STEX* dataset, some texture images are stationary, while some others appear as a collection of objects (Figure 5). In Figure 6, the CLP curves corresponding to *bush* and *wood* images are very similar with reduced magnitude in the difference spectra. Such behaviour corresponds to textures that are quiet homogeneous around each spatial location in accordance to the select neighbourhood radius. In another hand, the *bark* and *tree* images include more complex textures, inducing a biggest average colour difference between the neighbourhood centre and his periphery. The texture complexity induces also the magnitude variations for the middle and high frequencies.

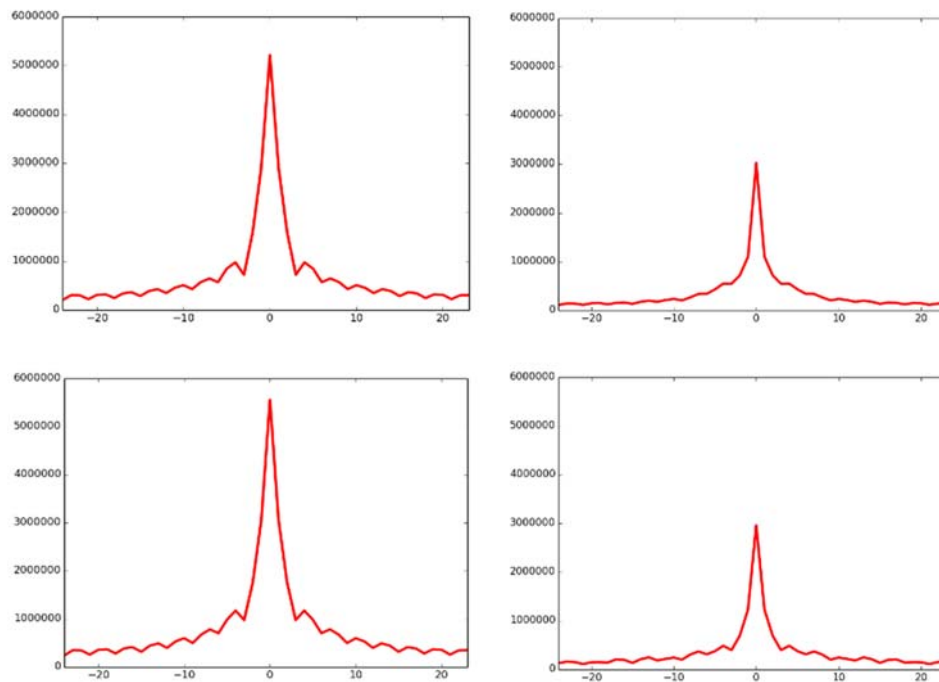


Figure 6: Colour local pattern amplitude from *STEX* test – *Bark 01* (top left), *Bush 08* (top right), *Tree 05* (bottom left) and *Wood 30* (bottom right).

CLP features for some ALOT images

ALOT is an impressive colour image collection of 250 distinct rough textures (some images are shown in the Figure 7), acquired by 4 different colour camera ($c=1, 2, 3, 4$). For each image and camera, six illuminations are considered ($I=1, 2, 3, 4, 5, 8$) and 4 rotations ($r=0^\circ, 60^\circ, 120^\circ, 180^\circ$) [23]. Three image sizes are proposed: full resolution (1536×1024) half resolution (768×536) and quarter resolution (384×256) pixels, all of them of 24 bits. Figure 8 shows that the average CLP curves for the three of the four images present a reduced energy, as for *wood* and *bush* cases in *STEX* images. The four texture signatures are clearly different. The most uniform ones in a perceptual point of view is the *ribbed cotton*

texture, as expected the average CLP curve presents the smallest variations at each frequency range. By opposition to the *moss* texture, for which the smallest variations (high spatial frequency range) are kept by the high frequencies in the average CLP curves.



Figure 7: Some images of colour texture from ALOT test; left to right – Tea, Ribbed cotton, Moss and Cotton wool (there are totally 250 images captured under the same illumination conditions but with different viewing conditions).

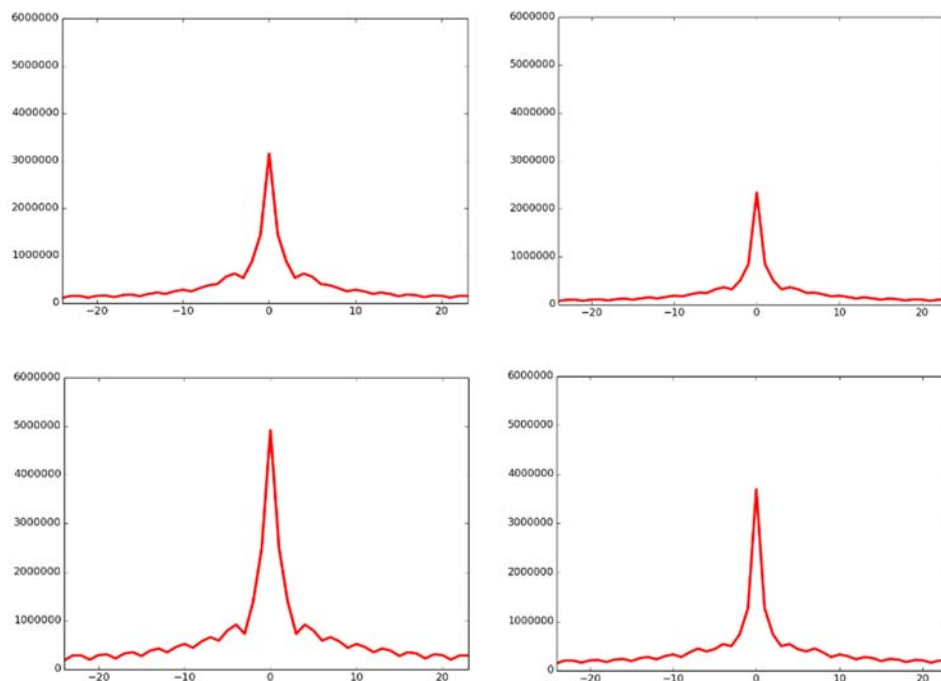


Figure 8: Colour local pattern amplitude from ALOT test – Tea (top left), Ribbed cotton (top right), Moss (bottom left) and Cotton wool (bottom right).

Inter-texture distance analysis

Before to address the performance of the CLP feature in texture classification, we analyse the intra and inter-class distance (L_2 form) in the CLP signature in order to assess their discrimination capacity. We consider each image I analysed previously as a class and the sub-images I_s as the class samples. Each sub-image is associated to the average signature $sig_{cpl\Delta}(I_s)$ and the class centre C_{cl} is defined by the average CLP signatures processed from the average signatures of the sub-images I_s . Then the distance intra-class d_{ic} is:

$$d_{ic} = \frac{1}{n} \sum_{I_s} d \left(sig_{cpl\Delta}(I_s), C_{cl}(I) \right) \quad (7)$$

$$\text{where } C_{cl} = \frac{1}{n} \sum_{I_s} sig_{cpl\Delta}(I_s)$$

The inter-class distance d_{inc} is the distance between two centres of class C_{cl} .

$$d_{inc} = d\left(C_{cl_i}(I), C_{cl_j}(I)\right) \quad (8)$$

In Tables 1 to 4, the diagonal represents the intra-class distance, and the cells out of diagonal the inter-class distance. It is expected that the intra-class distance be lowest than the inter-class distances. According to this hypothesis, good performances in texture classification would be obtained.

Table 1 shows the obtained distances for images from *OUTEX* database. Unfortunately some intra-class distances are higher than the inter-class distances (case of *Canvas 2* with *Canvas 4* and *Canvas 20* with *Wool 4*). This behaviour is directly correlated to the non-stationarity of the analysed textures and to the similarity between the textile structure (*Canvas 4* and *Canvas 20 b.e.*).

	Canvas 2	Canvas 4	Canvas 20	Wool 4
Canvas 2	7.26×10^{-6}	3.90×10^{-6}	11.04×10^{-6}	7.28×10^{-6}
Canvas 4	---	1.41×10^{-6}	7.06×10^{-6}	3.32×10^{-6}
Canvas 20	---	---	6.74×10^{-6}	3.78×10^{-6}
Wool 4	---	---	---	4.18×10^{-6}

Table 1: Intra- and inter-class L_2 distance for images of *OUTEX* database.

In the *VISTEX* database, the four intra-class distances are lowest than the inter-class distances (Table 2). The shape differences between the average CLP signatures and the texture stationarity explain this result.

	Food	Flower	Bark	Fabric
Food	10.65×10^{-6}	12.90×10^{-6}	27.04×10^{-6}	14.60×10^{-6}
Flower	---	5.53×10^{-6}	14.16×10^{-6}	16.69×10^{-6}
Bark	---	---	0.50×10^{-6}	30.80×10^{-6}
Fabric	---	---	---	7.07×10^{-6}

Table 2: Intra- and inter-class L_2 distance for images of *VISTEX* database.

The ration between the intra-class distances to the inter-class distances is important for the selected images of the *STEX* database (Table 3). We found one value very close in the distance between *bush* and *wood* class, than toward the centre of *bush* class. In Figure 6, the two average CLP signatures was very similar, and in Figure 5 we observed that the two texture images are relatively homogeneous inducing few intra-class variations explaining so the reduced intra-class distance.

	Bark	Bush	Tree	Wood
Bark	2.43×10^{-5}	29.37×10^{-5}	11.90×10^{-5}	29.74×10^{-5}
Bush	---	2.40×10^{-5}	17.95×10^{-5}	2.94×10^{-5}
Tree	---	---	6.70×10^{-5}	18.71×10^{-5}
Wood	---	---	---	2.68×10^{-5}

Table 3: Intra- and inter-class L_2 distance for images of *STEX* database.

Results for the selected images of *ALOT* database are presented in Table 4. The *tea* image cannot be easily differentiate from the *ribbed* and *moss* ones. Rather than no problems appear for the other cases. Such results is a direct consequence of the non-stationarity aspect of the *tea* texture image. The variations between two sub-images are more important than the variations between the CLP representing the class centres.

	Tea	Ribbed cotton	Moss	Cotton wool
Tea	1.97×10^{-5}	0.67×10^{-5}	1.08×10^{-5}	6.13×10^{-5}
Ribbed cotton	---	0.78×10^{-5}	1.68×10^{-5}	6.73×10^{-5}
Moss	---	---	0.88×10^{-5}	5.07×10^{-5}
Cotton wool	---	---	---	0.49×10^{-5}

Table 4: Intra- and inter-class L_2 distance for images of *ALOT* database.

Performance in classification

To compare the impact of the Colour Local Pattern (CLP) in front of other approaches of Local Binary Pattern (LBP) for colour images, we select the basic and complete classification scheme proposed by Arvis [12]. Then we compare CLP to grey-level based approaches for colour images. The first one combines a texture analysis adding its colour average (Grey-Level Approach with Colour Information: GLACI) and the second one extracts the relationship between the channels in a Cross-Channel Marginal Approach (CCMA) as proposed by Maempa [10]. Following this classification scheme, we develop our results on the two colour texture databases *OUTEX* (TC 00013, 68 textures), *VISTEX* (TC0006, 54 textures) as defined by Arvis. However we add *ALOT* (250 textures, 6 illuminates and 4 cameras) and *STEX* (476 textures) databases that include more complex texture images.

Table 5 shows that CLP obtains a higher rate of a good classification for 3 of the 4 evaluated databases (*VISTEX*, *STEX* and *ALOT*). A gain greater than 10% is obtained in the two databases having a more complex spatio-chromaticity (*STEX* and *ALOT*) [22].

	LBP-GLACI	LBP-CCMA	CLP	difference
OUTEX	85.70	80.73	82.10	-3.60
VISTEX	97.02	97.45	97.70	0.35
STEX	60.34	71.24	83.90	12.70
ALOT	58.30	70.64	81.30	11.30

Table 5: Good classification rate for grey-level approach with colour information in Local Binary Pattern (GLACI-LBP), Local binary pattern with colour information in cross-channel marginal approaches (LBP-CCMA) and colour local pattern (CLP).

Differences in classification performances are due to the inner content of the used databases. As previously explained *STEX* and *ALOT* contain more images from natural textures rather than in the *OUTEX* case where the textures comes essentially from man-made structures and is known as including few coloured structures. As *VISTEX* and *ALOT* databases include images from the nature, the texture content is more complex. This complexity is relative to multi-scale structures inside the images and to the strong correlations between the colour channels. Such colour correlation between the channels is naturally induced by the continuous response of the acquired content in the spectral domain and the

non-null intersection between the spectral sensitivities of the sensor channels. For such spatio-chromatic complexities, the colour local pattern approaches are well adapted, with an average gain of 13% in comparison to the *OUTEX* case.

The main differences in the CLP approach by opposition to the colour local binary approaches are in the colour consideration and in the detail preservation by removing the binarisation step. For the *OUTEX* database, the best performances are obtained with the GLACI approach (Grey-level approach using direct LBP on intensity image and adding some colour moment). In this case, the man-made content with basic textures including few variations in the colour content of each image and generally describe as monoscale textures justify the non-necessity of a more complex approach. In addition, more complex approaches will keep information at highest frequencies not discriminant for these texture (Gibbs phenomena).

Finally, Figure 9 shows some images for which the CLP fails in the texture classification task. These cases are interesting because the texture content is as in the *OUTEX* case: content defined in one or two monoscale structures (*Macaroni*, *Chips* for *ALOT* case and *Food*) and with few colour local variations.



Figure 9: Images from *ALOT* database that have problems in the classification percentage; left to right – *Macaroni* (coloured), *Macaroni* (penne), *Chips* (natural) and *Shabby*.

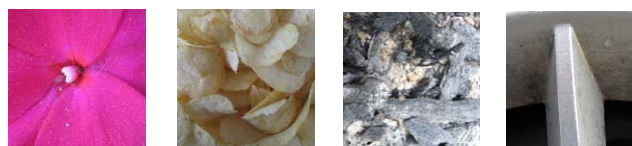


Figure 10: Images from *STEX* database that have problems in the classification percentage; left to right – *Flower 11*, *Food 01*, *Miscellaneous 01* and *Miscellaneous 43*.

Conclusions

Keeping the initial idea of the local binary pattern, we proposed a new expression adapted to colour domain. To obtain a feature coherent to the human vision and allowing to compare texture discrimination obtained by machine and human vision, we selected to base our construction on the colour differences processed in a perceptual colour space. The core of the feature is then the frequency representation of the colour difference sequences for a defined spatial neighbourhood.

Obtained signatures of Colour Local Pattern (CLP) are easy to interpret and help us to identify change trends in the textured and coloured content. Static and homogeneous textures present an important magnitude for the null frequency. In addition, this null frequency is directly correlated to the average perceptual colour difference between a pixel in the image and a neighbourhood at a fixed distance. For more heterogeneous and complex texture, the energy is transferred into the highest frequencies in relation to the ratio between the distance parameter and the texture pattern size.

Colour Local Pattern (CLP) approach is more interesting when the spatio-chromatic complexity of images increases. By opposition, basic approaches separating texture and colour are more adapted for

images of simple textures as in the *OUTEX* images. By opposition for textures coming from natural structures, as in the *STEX* and *ALOT* image cases, the gain in performance overpasses 10%.

Under another point of view, the CLP expression proposes an efficient implementation of the *texton* notion proposed by Julesz. The *texton* notion is embedded without the requirement to a segmentation process and adapted to texture characterisation/discrimination. The notion is limited to a circular neighbourhood but embed a spatial and perceptual colour distances. Such possibilities induces the future developments in progress. Firstly a set of psycho-physical experiments to assess the feature performances in texture discrimination and to express a full and vector expression for the Colour Local Pattern (CLP). The objective is to define how to embed the angular variation of the vector difference around the circular neighbourhood in the signature construction according to the human perception of the colour variations. Secondly, taking benefit of the relationship between the inner spatio-chromatic complexity of an image and the necessity to use a vector way to characterise the texture content, we are developing a multiscale construction to assess the spatio-chromatic complexity of images.

References

1. Landy MS and Graham N (2004), Visual perception of texture, in *The Visual Neurosciences*, Chalupa LM and Werner JS (eds.), MIT Press, Cambridge, MA, 1106-1118
2. Neisser U (1967), *Cognitive Psychology*, New York: Appleton-Century-Crofts.
3. Wandell BA (1995), *Foundations of Vision*, Sinauer Associates Inc.
4. Julesz B (1965), Texture and visual perception, *Scientific American*, **212**, 45-60.
5. Julesz B (1975), Experiments in the visual perception of texture, *Scientific American*, **232**, 20-30.
6. Caelli T and Julesz B (1978), On perceptual analyzers underlying visual texture discrimination: Part I, *Biological Cybernetics*, **28** (3), 167-175.
7. Julesz B and Bergen JR (1983), Textons: The fundamental elements in preattentive vision and perception of textures, *Bell System Technical Journal*, **62**, 1619-1645.
8. Haralick RM, Shanmugam K and Dinstein I (1973), Textural features for image classification, *IEEE Transactions on Systems, Man and Cybernetics*, **SMC-3** (6), 610-621.
9. Poirson AB and Wandell BA (1996), Pattern-color separable pathways predict sensitivity to simple colored patterns, *Vision Research*, **36** (4), 515-526.
10. Mäenpää T and Pietikäinen M (2004), Classification with color and texture: jointly or separately?, *Pattern Recognition*, **37**, 1629-1640.
11. Drimbarean A and Whelan P (2001), Experiments in colour texture analysis, *Pattern Recognition Letters*, **22** (10), 1161-1167.
12. Arvis V, Debain C, Berducat M and Benassi A (2004), Generalization of the co-occurrence matrix for colour images: Application to colour texture segmentation, *Image Analysis & Stereology*, **23**, 63-72.
13. Palm C (2004), Color texture classification by integrative co-occurrence matrices, *Pattern Recognition*, **37** (5), 965-976.
14. Martínez Ríos A, Ledoux A, Richard N and Fernandez-Maloigne C (2014), Colour Texture classification and spatio-chromatic complexity, *Proceedings of the X Conferenza del Colore*, 1-14, Genoa (Italy).
15. Martínez Ríos A, Richard N and Fernandez-Maloigne C (2015), Alternative to colour feature classification using colour contrast occurrence matrix, *Proceedings of the SPIE - Twelfth International Conference on Quality Control by Artificial Vision (QCVA)*, **9534** (File 9534 11), 1-9, At Le Creusot (France).
16. Ojala T, Pietikäinen M and Harwood D (1996), A comparative study of texture measures with classification based on feature distributions, *Pattern Recognition and Image Analysis*, **29** (1), 51-59
17. Porebski A, Vandenbroucke N and Hamad D (2013), LBP histogram selection for supervised color texture classification, *Proceedings of the 20th IEEE International Conference on Image Processing (IEEE-ICIP'13)*, 3239-3243, Melbourne (Australia).
18. Nanni L, Lumini A and Brahmam S (2010), Local binary patterns variants as texture descriptors for medical image analysis, *Artificial Intelligence in Medicine*, **49** (2), 117-125.
19. Yang F, Xu Y-Y, Wang S and Shen H (2014), Image-based classification of protein subcellular location patterns in human reproductive tissue by ensemble learning global and local features, *Neurocomputing*, **131**, 113-123.

20. Huang D, Shan C, Ardabili M, Wang Y and Chen L (2011), Local binary patterns and its application to facial image analysis: A survey, *Proceedings of the IEEE Transactions on Systems, Man, and Cybernetics, Part C: Applications and Reviews*, **41** (6), 765-781.
21. Pietikäinen M, Guoying Z, Hadid A and Ahonen T (2011), *Computer Vision using Local Binary Pattern*, London: Springer.
22. Hossain S and Serikawa S (2013), Texture databases - a comprehensive survey, *Pattern Recognition Letters*, **34** (15), 2007-2022.